EXPERIMENTAL MEASUREMENTS OF CRACK GROWTH RESISTANCE CURVES FOR A PIPELINE STEEL USING SE(T) FRACTURE SPECIMENS

Roberto Piovatto, betaopiovatto@gmail.com
Waldek W. Bose Filho, waldek@sc.usp.br
Dirceu Spinelli, dspinell@sc.usp.br
Department of Materials and Aeronautical Engineering, EESC
University of São Paulo, São Carlos, SP 13566-590, Brazil

Eduardo Hippert Jr., hippert@petrobras.com.br
Petrobrás – CENPES - TMEC
Rio de Janeiro, RJ 21949-900, Brazil

Sebastian Cravero, scravero@gmail.com
Claudio Ruggieri, claudio.ruggieri@poli.usp.br
Department of Naval Architecture and Ocean Engineering, PNV-EPUSP
University of São Paulo, São Paulo, SP 05508–900, Brazil

Abstract *– This work presents an investigation of the ductile tearing properties for an API 5L X60 pipeline steel using experimentally measured crack growth resistance curves (*J-R *curves). Use of these materials are motivated by the increasing demand in the number of applications for manufacturing high strength pipes for the Brazilian oil and gas industry including marine applications and steel catenary risers. Testing of the pipeline steels employed side-grooved SE(T) specimen with varying crack size to determine the* J-R *curves based upon the unloading compliance method using a single specimen technique. Recent developed compliance functions and* eta*-factors applicable for SE(T) fracture specimens are introduced to determine crack growth resistance data from laboratory measurements of load-displacement records. This experimental characterization provides additional toughness data which serve to evaluate crack growth resistance properties of pipeline steels using SE(T) specimens with varying geometries.*

Keywords*: ductile fracture, structural integrity, J-R curve, pipeline steel, SE(T) specimen*

1. INTRODUCTION

The accurate prediction of fracture behavior for oil and gas pipelines with crack-like flaws is essential in fitness-for-service (FFS) methodologies (such as, for example, repair decisions and life-extension procedures) and to ensure fail-safe operations which avoid costly leaks and ruptures due to material damage caused by structural defects. For high strength pipeline steels, the material failure (leakage or sudden rupture) is most often preceded by large amounts of slow, stable crack growth. Under sustained ductile tearing of the (macroscopic) crack-like defect, large increases in the load-carrying capacity of the structure, as characterized by J resistance curves (J-R curves), are possible beyond the limits given by the crack driving force at the onset of crack growth. Advanced procedures for structural integrity of ductile pipelines incorporate the increase in toughness of these materials during ductile crack growth by comparing the structure's crack driving force with the material's crack growth resistance (Hutchinson, 1983; Zerbst *et al.*, 2000; Anderson, 2005).

Conventional testing standards to measure J resistance curves most often employ three-point bend SE(B) and compact tension C(T) specimens containing deep, through cracks ($a/W \geq 0.5$). However, structural defects (e.g., blunt corrosion, slag and nonmetallic inclusions, weld cracks, dents at weld seams, etc.) in pressurized piping systems are very often surface cracks that form during fabrication or during in-service operation (Eiber and Kiefner, 1986; AWS, 1987; NEB, 1996). These crack configurations generally develop low levels of crack-tip stress triaxiality which contrasts sharply to conditions present in deeply cracked specimens. Recent defect assessment procedures advocate the use of geometry dependent fracture toughness values so that crack-tip constraint in the test specimen closely matches the crack-tip constraint for the structural compo-

nent. In particular, J resistance curves measured using single edge notch tension (SE(T)) specimens appear more applicable for characterizing the ductile tearing properties of pressurized pipelines and cylindrical vessels than standard, deep notch fracture specimens under bend loading. The primary motivation to use SE(T) fracture specimens in defect assessment procedures of cracked pipes is the strong similarity in crack-tip stress and strain fields which drive the fracture process for both crack configurations. In particular, Cravero and Ruggieri (2005) and Silva *et al.* (2006) demonstrated that pin-loaded SE(T) fracture specimens and axially cracked pipes with common crack sizes relative to pipe wall thickness and specimen width display essentially similar levels of crack-tip constraint under the same macroscopic loading as measured by J.

However, full understanding of the fracture behavior directly connected to this crack configuration which supports development of standard test procedures is still lacking. Joyce *et al.* (1993) and Joyce and Link (1995) examined the ductile tearing behavior of structural steels using SE(T) fracture specimens and developed approximate techniques to estimate crack growth resistance curves based upon the unloading compliance method. While their work demonstrated the capability of unloading compliance procedures to evaluate J-R curves for crack geometries under predominantly tensile loading, rather little further effort was expended following their work in systematic investigation and standardization aspects of the SE(T) configuration. In particular, the accurate determination of crack-tip driving forces (as measured by J) and crack extension becomes central in robust correlations of fracture conditions between these test specimens and structures.

This work presents an investigation of the ductile tearing properties for an API 5L X60 pipeline steel using experimentally measured crack growth resistance curves (J-R curves). Use of these materials are motivated by the increasing demand in a number of applications for manufacturing high strength pipes for the Brazilian oil and gas industry including marine applications and steel catenary risers. Testing of the pipeline steels employed side-grooved SE(T) specimen with varying crack size to determine the J-R curves based upon the unloading compliance method using a single specimen technique. Recently developed compliance functions and *eta*-factors applicable for SE(T) fracture specimens are introduced to determine crack growth resistance data from laboratory measurements of load-displacement records. This experimental characterization provides additional toughness data which serve to evaluate crack growth resistance properties of pipeline steels using SE(T) specimens with varying geometries.

2. MATERIAL DESCRIPTION

The material used in this study is a high strength, low alloy (HSLA) API 5L-X60 (API, 200o) used in oil and gas pipelines. The steel is control-rolled in the temperature range of 720–760°C to obtain fine and/or highly deformed (pancaked) austenite grains, which transform into small ferrite grains during cooling thereby greatly enhancing toughness while improving yield strength (Knott and Harrison, 1984). Metallographic examination of an etched surface of the API-X60 steel revealed a layered microstructure aligned with the plate rolling direction, with refined grains of ferrite and colonies of pearlite. Figure 1 shows the steel microstructure in the longitudinal, transverse and through-thickness directions. Investigation of the inclusions by image analysis of polished surfaces revealed a very low volume fraction of globular oxide particles. Table 1 lists the chemical composition of the tested material which displays low C content relative to common pressure vessel and structural steels but with the addition of small amounts of Nb, V and Ti; good toughness properties and low transition temperature may thus be anticipated.

Table 1 Chemical composition of API 5L-X60 steel (wt.%)

C	Si	Mn	P	Al	B	S	Nb	V	Ti	Pb	Ni
0.11	0.26	1.44	0.028	0.028	0.0003	0.007	0.04	0.044	0.013	0.003	0.02

Mechanical tensile tests, conducted on standard tensile specimens (5 mm diameter) extracted from the transverse plate direction (thickness of 15 mm), provide the room temperature (20ºC) stress-strain data. These test pieces were loaded in a 25 ton hydraulic testing machine fitted with axial extensometers according to ASTM E8M (ASTM, 2000a) requirements. Table 2 also summarizes the mechanical properties obtained from these tests. The material has $\approx$ 499 MPa yield stress (σ_{ys}) with relatively moderate strain hardening (σ_u/σ_{ys} = 1.25, where σ_u denotes the ultimate tensile strength). These tensile test results are in accordance with the requirements prescribed by API specification (API, 2000). Figure 2(a) shows the engineering stress-strain curves at test temperature for the steel. Other mechanical properties for this material include Young's modulus, $E = 207$ GPa and Poisson's ratio, $\nu = 0.3$.

A set of 10 Charpy-V (CVN) impact specimens (T-L orientation) was tested in a 360 J full-scale Tinius-Olsen pendulum machine, following the requirements of ASTM E23 standard (ASTM, 2000b). Test pieces were broken in 5 different temperatures: -100°C, -80°C, -60°C, -40°C and 20°C. Figure 2(b) shows the measured absorbed energy with test temperature for the X60 steel. At room temperature (20°C) this material exhibits fully ductile fracture so that transition effects are not considered in the fracture mechanics testing results.

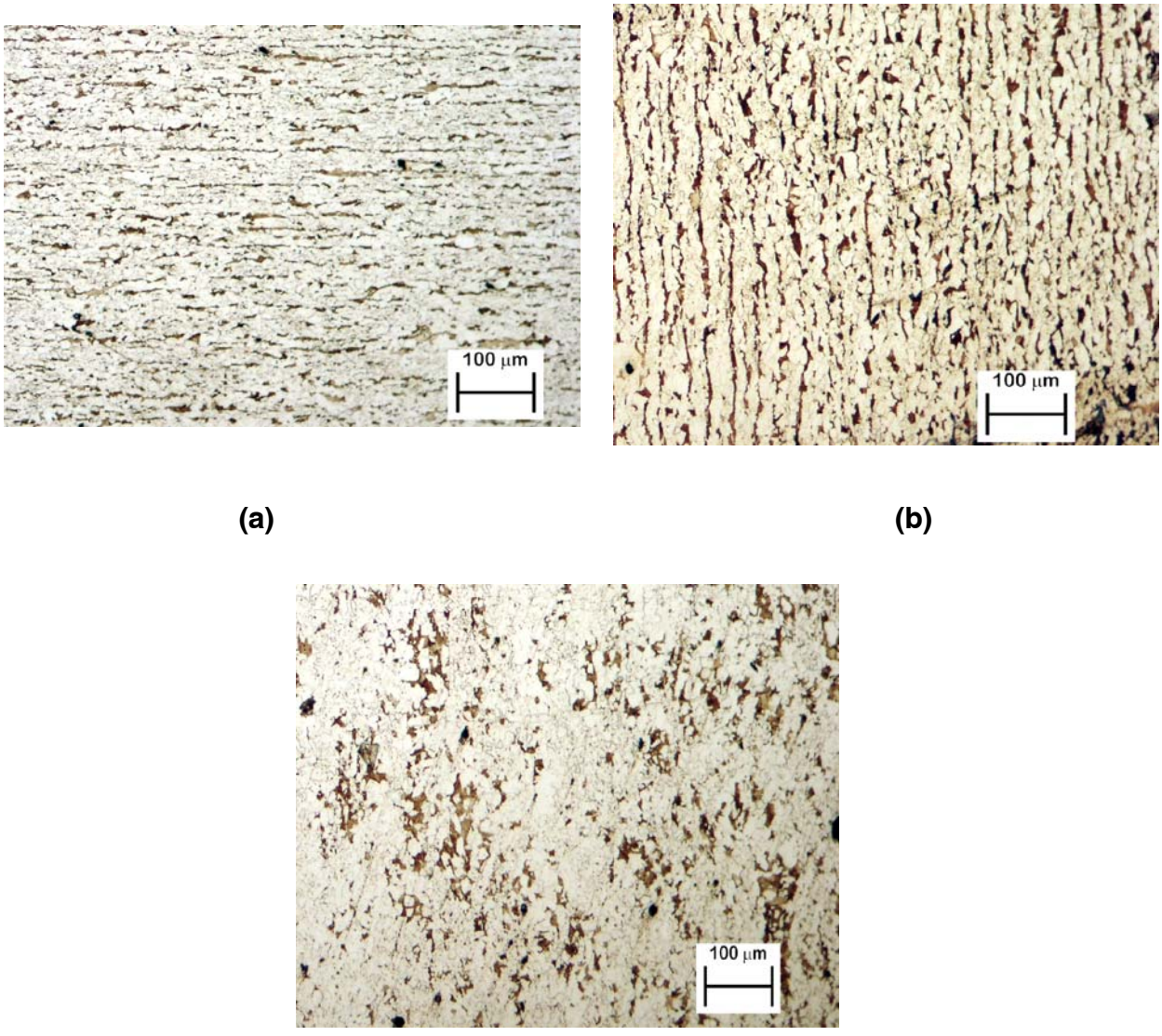

Figure 1 *Microstructure of API 5L X60 Steel; a)Longitudinal direction; b) Transverse direction and c) Through-thickness direction.*

Table 2 Mechanical properties of API 5L-X60 steel (20°C)

Specimen	Orientation	σ_{ys} (MPa)	σ_u (MPa)	Elongation (%)
CP 01	Transversal	501.5	631.5	18.3
CP 02	Transversal	496.8	618.5	24.3
Average	–	499.1	625.0	21.3

3. FRACTURE TOUGHNESS TESTING

Single edge notch specimens under tension – SE(T) specimens – with a fixed overall geometry and varying crack length to width ratios, a/W were extracted from the plate in the T-L position. The specimens have thickness $B = 12.5$ mm, width $W = 32$ mm, pin-loading span $H = 214$ mm ($H/W \approx 6.7$) and crack length to width ratio $a/W = 0.5$ and 0.2. Figure 3(a) provides an schematic illustration of specimen geometry and dimensions.

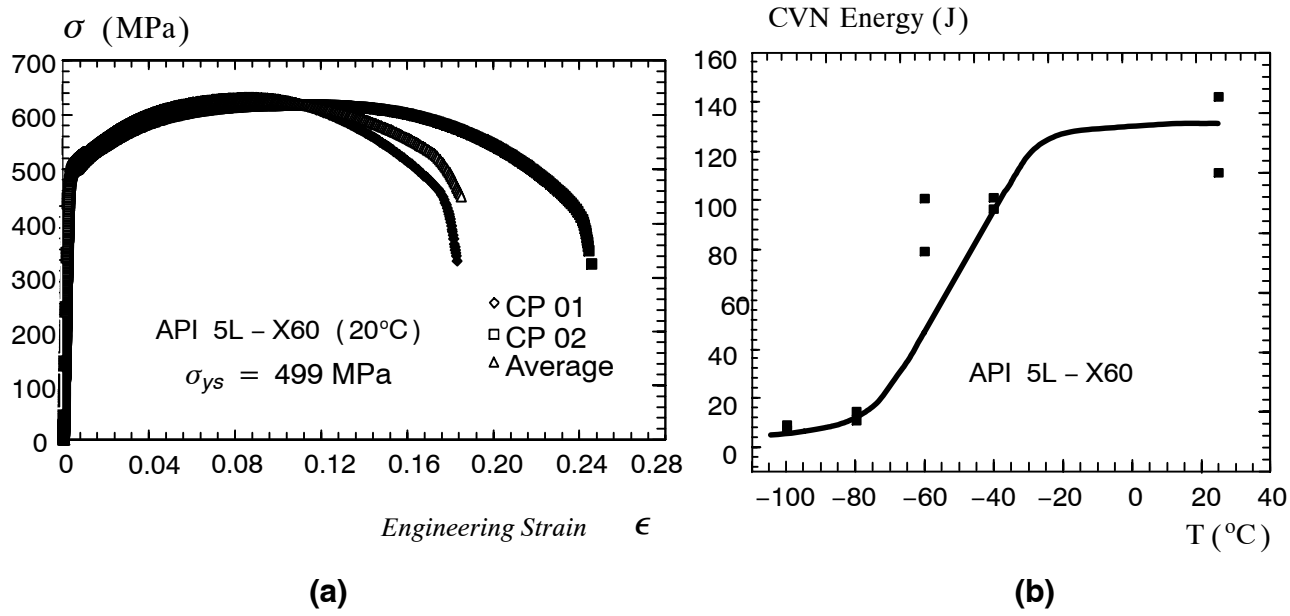

Figure 2 *(a) Engineering stress–strain curve for X60 steel; (b) CVN transition curve for API–X60 steel.*

The SE(T) specimens were precracked in bending using a three-point bend apparatus very similar to a conventional three-point bend test (see Fig. 3(b)). After fatigue precracking, the specimens were side-grooved to a net thickness of ~80% the plate thickness (10% side-groove on each side) to promote uniform crack growth and tested following some general guidelines described in ASTM E1820 standard (ASTM, 2001). Here, we note that the SE(T) specimen is not standardized; consequently, different analytical equations that those provided in the ASTM standard were utilized to estimate the applied *J*-values and the crack length from the measured specimen compliance as described next.

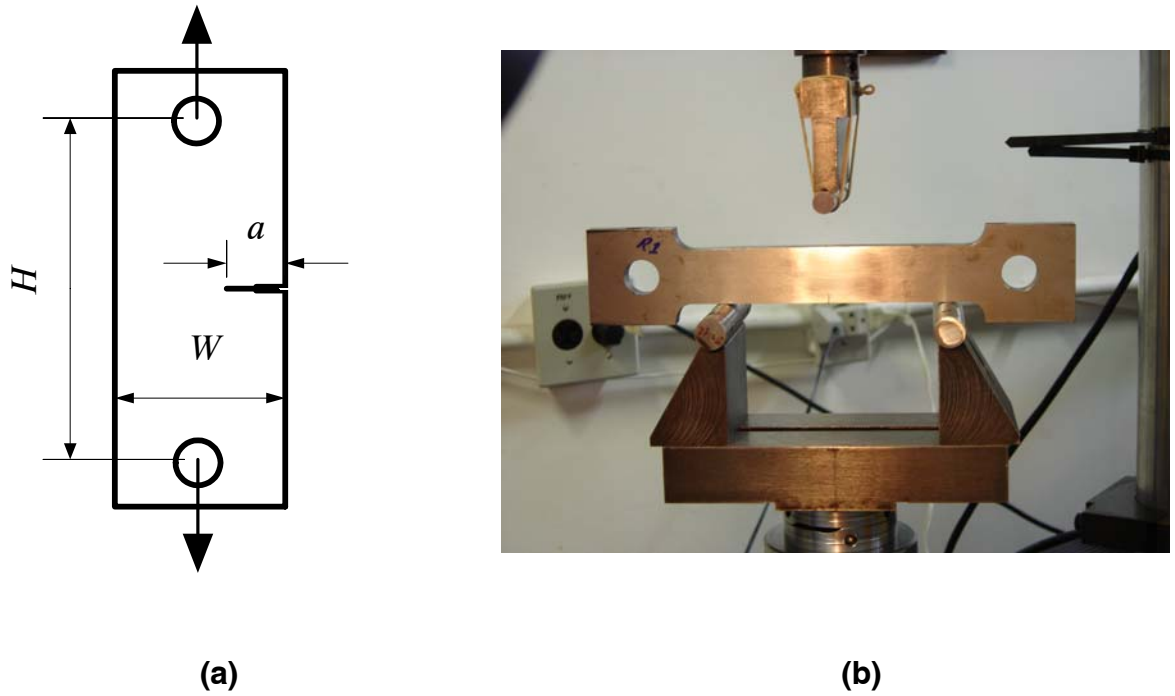

Figure 3 *(a) Geometry of SE(T) fracture specimen; (b) Fatigue precrack test rig for bend loading.*

4. ESTIMATION PROCEDURE OF J-R CURVES

Experimental efforts to support the development of laboratory measurements for fracture toughness resistance data have focused primarily on the unloading compliance method based upon testing of a single specimen (Anderson, 2005; Joyce

et al., 1993, Joyce and Link, 1995; Saxena, 1998). Implementation of the method essentially follows from determining the instantaneous value of J and specimen compliance at partial unloading during the measurement of the load-displacement curve for the tested cracked configuration. The technique then enables accurate estimations of J and Δa at several locations on the load-displacement records from which the J-R curve can be developed. The procedure to estimate crack growth resistance data for the tested SE(T) specimens derives from the work of Cravero and Ruggieri (2007a, 2007b). Here, we present only a summary of the methodology and provide the key equations to calculate the J-integral and crack growth from measured load-displacement data.

Upon consideration of the elastic and plastic contributions to the strain energy for a cracked body under Mode I deformation (Anderson, 2005), J can be conveniently defined in terms of its elastic component, J_{el}, and plastic component, J_{pl}, as

$$J = J_{el} + J_{pl} = \frac{K_{\mathrm{I}}^2}{E'} + \frac{\eta_J A_{pl}}{B_N b_0} \tag{1}$$

where K_{I} is the elastic stress intensity factor for the cracked configuration, A_{pl} is the plastic area under the load-displacement curve, B_N is the net specimen thickness at the side groove roots ($B_N = B$ if the specimen has no side grooves where B is the specimen gross thickness), b_0 is the initial uncracked ligament ($b_0 = W - a_0$ where W is the width of the cracked configuration and a_0 is the initial crack length). In writing the first term of Eq. (1), plane-strain conditions are adopted such that $E' = E/(1-\nu^2)$ where E and ν are the (longitudinal) elastic modulus and Poisson's ratio, respectively. Factor η_J introduced by Sumpter and Turner (1976) represents a nondimensional parameter which relates the plastic contribution to the strain energy for the cracked body and J. For definiteness, these quantities are denoted η_J^{CMOD} and η_J^{LLD}. While both definitions serve essentially as a means to quantify the effect of plastic work on the J-integral, η_J-values based on *LLD* have a different character than the corresponding η_J-values based on *CMOD*. The present work adopts η_J-values based on *CMOD* to determine the J-R curve for the tested material.

The previous expression (1) defines the key quantities driving the evaluation procedure for J as a function of applied (remote) loading and crack size. Further, the previous solution for J_{pl} retains strong contact with the deformation plasticity definition of J and thus assumes nonlinear elastic material response. However, the area under the actual load-displacement curve for a growing crack differs significantly from the corresponding area for a stationary crack (which the deformation definition of J is based on) (Anderson, 2005). Consequently, the measured load-displacement records must be corrected for crack extension to obtain an accurate estimate of J-values with increased crack growth. A widely used approach (which forms the basis of current standards such as ASTM E1820 (2001)) to evaluate J with crack extension follows from an incremental procedure which updates J_{el} and J_{pl} at each partial unloading point, denoted k, during the measurement of the load *vs.* displacement curve in the form

$$J_k = J_{el}^k + J_{pl}^k \quad . \tag{2}$$

Within this approach, the k-th elastic term of J is directly calculated from the corresponding k-th value of K_{I} using the first term of previous Eq. (1) which yields

$$J_{el}^K = \frac{\left(K_{\mathrm{I}}^k\right)^2}{E'} \quad . \tag{3}$$

For the SE(T) specimen, parameter K_{I} is evaluated at the current load, P_k, as

$$K_{\mathrm{I}}^k = \frac{P_k}{B_N \sqrt{W}} \mathcal{F}\left(a_k/W\right) \tag{4}$$

where $\mathcal{F}\left(a_k/W\right)$ defines a nondimensional stress intensity factor dependent upon specimen geometry, crack size and loading condition. Cravero and Ruggieri (2007a) provide analytical expressions for the nondimensional stress intensity factors $\mathcal{F}\left(a_k/W\right)$ for the SE(T) specimens analyzed here, .

Similarly, the k-th plastic term of J follows from the second term of Eq. (1) using the current plastic area, A_{pl}^k. Given an estimated value for J_{pl} at $k-1$, the k-th value of J is given by

$$J_{pl}^k = \left[J_{pl}^{k-1} + \frac{\eta_{k-1}}{b_{k-1} B_N} \left(A_{pl}^k - A_{pl}^{k-1} \right) \right] \times \Gamma \tag{5}$$

in which Γ is defined as

$$\Gamma = 1 - \frac{\gamma_{k-1}}{b_{k-1}}\left(a_k - a_{k-1}\right) \tag{6}$$

where factor γ is evaluated from

$$\gamma_{k-1} = \left[-1 + \eta_{k-1} - \left(\frac{b_{k-1}}{W}\frac{\eta'_{k-1}}{\eta_{k-1}}\right)\right] \tag{7}$$

with

$$\eta'_{k-1} = W\frac{d\eta_{k-1}}{da_{k-1}} \quad . \tag{8}$$

Another key step in the experimental evaluation of crack growth resistance response involves the accurate estimation of the instantaneous crack length as testing progresses. The unloading compliance technique provides a convenient and yet simple procedure to correlate crack extension to the specimen compliance with increased crack growth. Cravero and Ruggieri (2007a) illustrate the essential features of the method. The slope of the load-displacement curve during the *k*-th unloading defines the instantaneous specimen compliance, denoted $\mathbb{C}_k$, which depends on specimen geometry and crack length.

Application of the procedure outlined above requires correct specification of all quantities entering directly into the calculation of *J* through Eq. (2-8) as well as the specimen compliance, $\mathbb{C}$. These quantities thus play a crucial role in defining the *J-R* curve from laboratory measurements of load *vs.* displacement for the tested specimen. Current test standards provide appropriate forms for factors η, γ and the compliance $\mathbb{C}$ which are only applicable to C(T) and SE(B) specimens with deep cracks ($a/W \geq 0.45$). The relatively limited analyses and data available to construct crack growth resistance data for SE(T) specimens underscores the need for improved and accurate descriptions of factors η, γ and compliance $\mathbb{C}$ for these crack configurations. Cravero and Ruggieri (2007a) provide detailed numerical and validation analyses which lead to a definite set of expressions describing those key quantities.

4.1 Compliance Correction Due to Rotation

The specimen compliance, $\mathbb{C}$, needed to determine the crack length may not reflect changes in specimen geometry due to large rotations as the test progresses for the pin-loaded SE(T) specimen displayed in Fig. 3(a). Specimen rotation shifts the measurement points for the applied load and *CMOD* with reference to the original (undeformed) configuration upon which the specimen compliance, C, is based on. By assuming a fixed position for the center of rotation, denoted by point O in Fig. 4, the crack mouth opening displacement and applied load are corrected for the effect of specimen rotation to yield the corrected specimen compliance in the form

$$\mathbb{C}_c^{CMOD} = \frac{\mathbb{C}_m^{CMOD}}{\left[\cos\theta - \frac{D\tan\theta}{2(R_C+z)}\right]\left[\cos\theta - \frac{H\sin\theta}{2r_2}\right]} \tag{9}$$

in which it is understood that subscripts *m* and *c* denote the measured and corrected quantities.

The correction of the measured load for the effect of specimen rotation is obtained by equating the applied moments about the rotation point *O* for the deformed and undeformed configurations (see Fig. 4(a)). Consequently, the measured load, P_m, and the corrected load, P_c, are then related by

$$P_c r_1 = P_m r_2 \tag{10}$$

in which the distances r_1 and r_2 are defined as

$$r_2 = r_1\cos\theta - \frac{H}{2}\sin\theta \tag{11}$$

with r_1 given by

$$r_1 = R_C - (W/2) \quad . \tag{12}$$

In the above expressions, the rotation angle, θ, is given by

$$\sin(\theta + \phi) = \frac{(V_m/2) + D}{\sqrt{D^2 + (R_C + z)^2}} \tag{13}$$

where

$$\phi = \arctan\left(\frac{D}{R_C + z}\right) \quad . \tag{14}$$

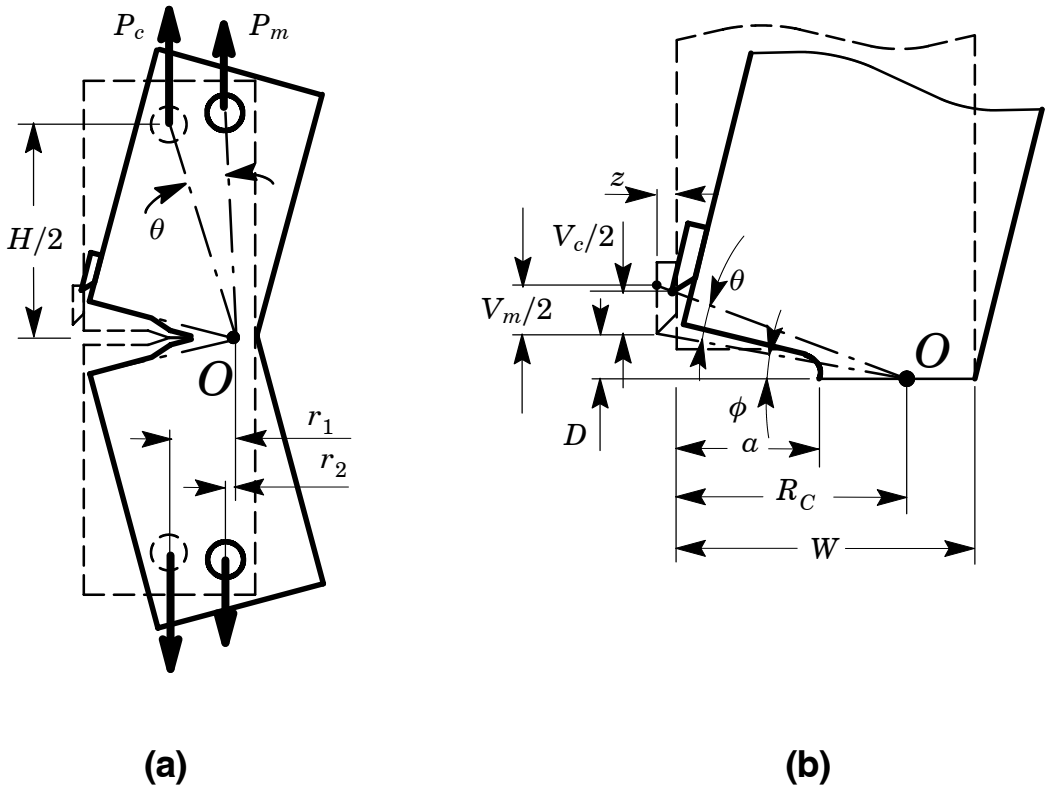

Figure 4 *Scheme of the rotation correction for the SE(T) specimen compliance: (a) shifting of the measurement point for the applied load; (b) shifting of the measurement point for CMOD.*

The rotation correction for the specimen compliance just presented clearly reveals the importance of the accurate choice for the position of the center of rotation, R_C. This geometric dimension can also be conveniently expressed by the sum of crack length and a fraction of the remaining crack ligament in the form $R_C = a + r_p(W - a)$ where r_p denotes the plastic rotation factor (see Fig. 4). Figure 5(a-b) shows the variation of the plastic rotation factor with increased *CMOD* normalized by the remaining crack ligament, $b = (W - a)$, for deeply ($a/W = 0.5$) and shallow ($a/W = 0.2$) cracked SE(T) specimens with $H/W = 6$ and varying strain hardening properties ($n = 5$, 10 and 20). The r_p-factor depends rather strongly on strain hardening for the shallow cracked SE(T) specimen, particularly for values of $CMOD/b \geq 0.01$. In contrast, the r_p-factor is fairly independent of strain hardening for the deeply cracked SE(T) specimen; here, after a transitional behavior for values of $\text{CMOD}/b \leq 0.03 \sim 0.04$, the r_p-factor attains a fixed value of ≈ 0.65.

5. *J-R* TESTING OF A PIPELINE STEEL

This section describes the evaluation of ductile tearing properties for a pipeline steel from laboratory measurements of load and CMOD for pin-loaded SE(T) specimens. Conducted as part of a collaborative program between the University of São Paulo and Petrobrás, testing of this specimen focuses on development of accurate procedures to evaluate crack growth resistance data for cracked pipelines and test techniques as needed for SE(T) crack configurations.

Bose and co-workers (2007) conducted unloading compliance tests at room temperature on pin-loaded, side-grooved SE(T) specimens of an API X60 steel in the T-L orientation. The specimens have a/W-nominal = 0.2 and 0.5 and $H/W = 6.7$ with thickness $B = 12.5$ mm, width $W = 32$ mm and pin-load distance $H = 214$ mm (refer to Fig. 3). Figure 6 shows the measured load-displacement curves (as described by *CMOD*) for the shallow and deep cracked test specimens.

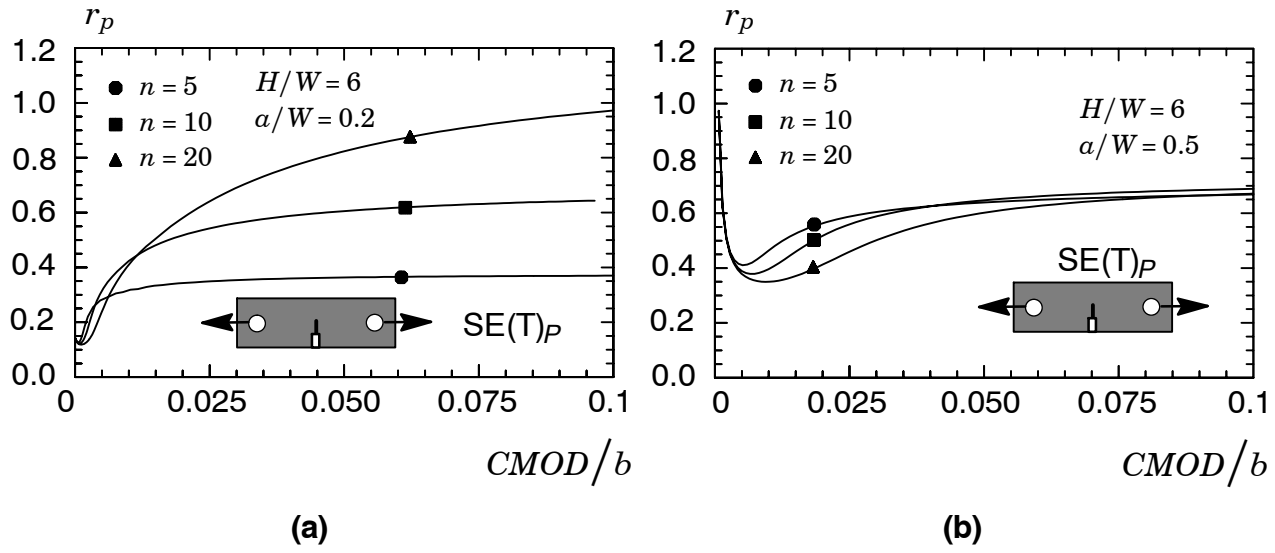

Figure 5 *Variation of plastic rotation factor, r_p, with increased CMOD for pin-loaded SE(T) specimens with H/W=6: a) a/W=0.2 and ; b) a/W=0.5.*

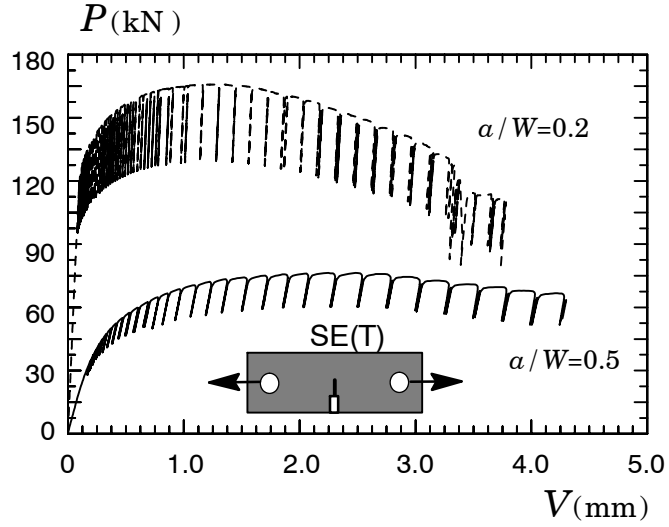

Figure 6 *Measured load-CMOD curves for the tested X60 steel using pin-loaded SE(T) specimen with varying crack sizes.*

Evaluation of the crack growth resistance curve follows from determining J and Δa at each unloading point of the measured load-displacement data. Based upon the results for the *eta*-factors developed by Cravero and Ruggieri (2007a), the present analysis employs η_J^{CMOD} to estimate the plastic component of the J-integral, J_{pl}. Further, the previous developed rotation correction is also utilized to correct the *CMOD* compliance for the strong bend moment (and the associated rigid body rotations) which develops in pin-loaded SE(T) specimens with increased crack growth.

Figure 7 displays the crack growth resistance curves for the tested material. The essential features of ductile tearing behavior are correctly captured within the estimation scheme just developed in which the resistance curve rises steadily and rather rapidly with increased crack growth. Such behavior is entirely consistent with previous results obtained by Joyce and Link (1995) for pressure vessel and structural steels.

Laboratory testing of deep crack ($a/W = 0.5$) 0.5(T) side-grooved compact tension specimens with thickness $B = 13$ mm was also conducted to measure the tearing resistance curves (J vs. Δa) at room temperature (20°C) for the API X60 pipeline steel (Petrobrás, 2002). These 0.5(T) C(T) specimens were tested at room temperature using a direct potential (DP) method to measure the crack growth resistance for the material. After fatigue pre-cracking, the specimens were side-grooved to a depth of 1 mm on each side to promote uniform crack growth over the thickness. Figure 8 presents the experimentally measured J vs. Δa curves. The fracture tests followed the procedures of ASTM Standard Test Method for Determining J-R Curves (E1820). Experimental J-values are determined using the measured load-load line displacement records. A direct

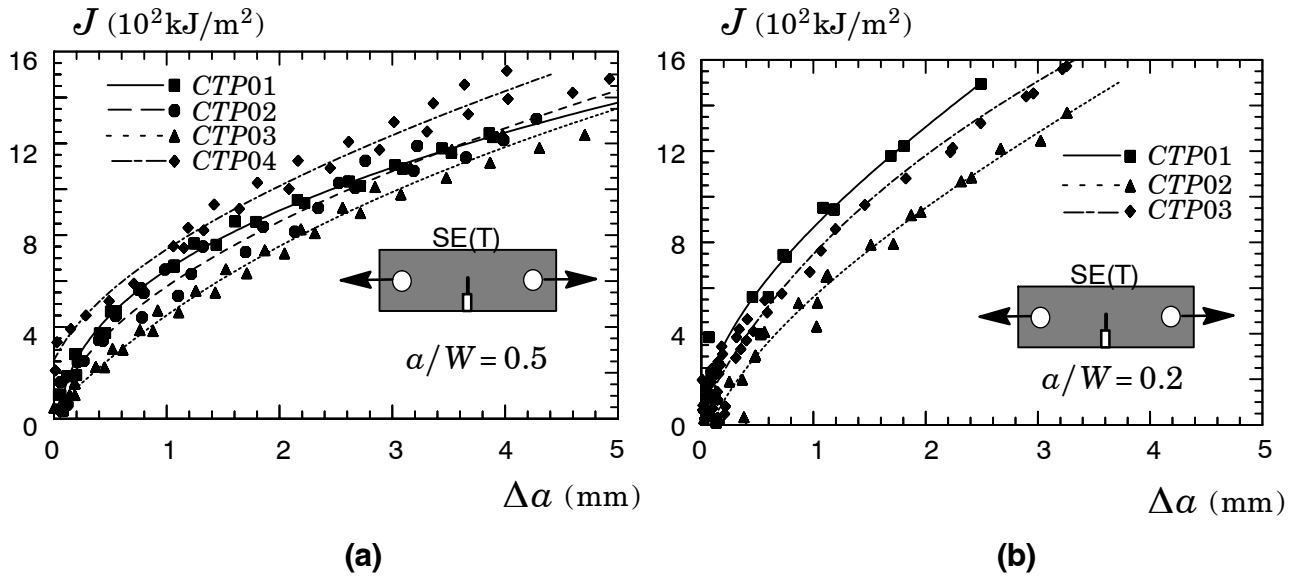

Figure 7 *Comparison of experimental resistance curves for deeply cracked SE(T) specimens; Comparison of experimental resistance curves for shallow cracked SE(T) specimens.*

comparison of the results shown in Fig. 8 with the J vs. Δa values displayed in previous Fig. 7 also provide strong support to the methodology outlined here for determining resistance curves based upon SE(T) fracture specimens. For a given amount of ductile tearing resistance, the J-values for the deeply cracked C(T) specimen are lower that the corresponding J-values for the deeply cracked SE(T) specimens. Such behavior is entirely consistent with experimental observations and arise from the loss of crack-tip constraint which develop in the SE(T) specimen as deformation progresses.

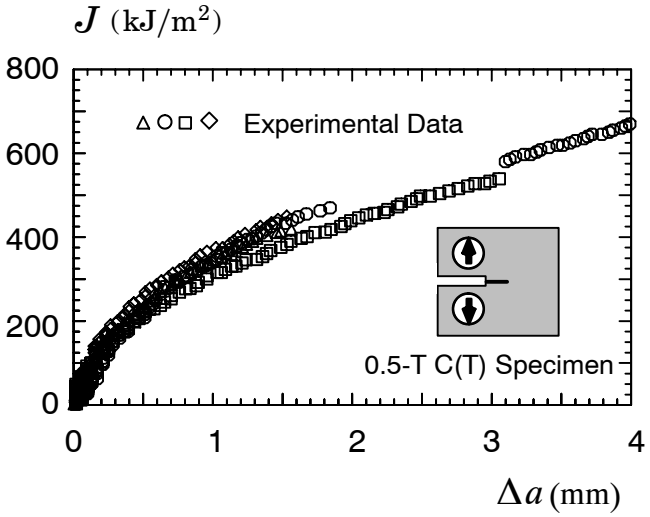

Figure 8 *Experimental R – curve for side-grooved 0.5-T C(T) specimen of API 5L-60 (20° C) (Petrobrás, 2002).*

6. CONCLUDING REMARKS

This study presents an experimental investigation and estimation procedure to evaluate crack growth resistance properties for a pipeline steel based upon SE(T) specimens. The experiments and analyses described provide a strong support to use unloading compliance methods to measure *J-R* curves for nonstandard SE(T) specimens with varying crack sizes subjected to predominantly tensile loading. Further, the exploratory validation analyses using experimentally measured load-displacement data for shallow and deeply-cracked SE(T) specimen made of an API X60 pipeline steel demonstrates the capability of the procedure in describing ductile tearing properties for the tested material. While additional experimental studies are needed to build a more extensive body of laboratory data, the results presented here provide a definite basis to support developments of standard test procedures for SE(T) specimens applicable in measurements of crack growth resistance data.

7. ACKNOWLEDGMENTS

This investigation is supported by Fundação de Amparo à Pesquisa do Estado de São Paulo (FAPESP) through Grant 03/02735-6. The authors acknowledge the Brazilian State Oil Company (Petrobrás) for making available the SE(T) fracture specimens used in testing of the API 5L X60 pipeline steel plate.

8. REFERENCES

American Welding Society (AWS), 1987, "Welding Handbook: Welding Technology", Eighth Edition, Vol. 1, Miami.

Anderson, T. L., 2005, "Fracture Mechanics: Fundaments and Applications - 3rd Edition", CRC Press, Boca Raton.

API 5L , 2000, "Specification for Line Pipe", American Petroleum Institute API, 42nd edition.

ASTM E8M–00b, 2000, "Standard Test Methods for Tension Testing of Metallic Materials [Metric]", American Society for Testing and Materials.

ASTM E23–00, 2000, "Standard Test Methods for Notched Bar Impact Testing of Metallic Materials", American Society for Testing and Materials.

ASTM E1820, 2001, "Standard Test Method for Measurement of Fracture Toughness", American Society for Testing and Materials.

Bose, W., Spinelli, D., Piovatto, R., Cravero, S. and Ruggieri, C., 2007, "Experimental Measurements of Crack Growth Resistance Curves for an API X60 Steel Using SE(T) Specimens", Manuscript in Preparation.

Cravero, S. and Ruggieri, C., 2005, "Correlation of Fracture Behavior in High Pressure Pipelines with Axial Flaws Using Constraint Designed Test Specimens - Part I: Plane-Strain Analyses," *Engineering Fracture Mechanics*, **72**, pp. 1344-1360.

Cravero, S. and Ruggieri, C., 2007a, "Estimation Procedure of *J*-Resistance Curves for SE(T) Fracture Specimens Using Unloading Compliance," *Engineering Fracture Mechanics* (In Press).

Cravero, S. and Ruggieri, C., 2007b, "The Unloading Compliance Procedure for *J-R* Curve Testing Using SE(T) Fracture Specimens," 19th International Congress of Mechanical Engineering, COBEM 2007.

Eiber, R. J. and Kiefner, J. F., 1986, "Failure of Pipelines", in Metals Handbook, Ninth Edition, Vol. 11 - Failure Analysis and Prevention, American Society for Metals, pp. 695-706.

Hutchinson, J.W., 1983, ''Fundamentals of the Phenomenological Theory of Nonlinear Fracture Mechanics.'' *Journal of Applied Mechanics*, Vol. 50, pp. 1042-1051.

Joyce, J. A., Hackett, E. M. and Roe, C., 1993, "Effects of Crack Depth and Mode Loading on the *J-R* Curve Behavior of a High Strength Steel," *Constraint Effects in Fracture, ASTM STP 1171*, E. M. Hackett, et al. Eds., American Society for Testing and Materials, Philadelphia, pp. 239-263.

Joyce, J. A., and Link R. E., 1995, "Effects of Constraint on Upper Shelf Fracture Toughness," *Fracture Mechanics, 26th Volume, ASTM STP 1256*, W. G. Reuter, et al. Eds., American Society for Testing and Materials, Philadelphia, pp. 142-177.

Knott, J.F. and Harrison, J.D., 1984, "Fundamentals of Fracture in Pipelines", Proceedings of International Seminar Fracture in Gas Pipelines, pp. 01-26, Moscow.

Koppenhoefer, K., Gullerud, A., Ruggieri, C., Dodds, R. and Healy, B., 1994, ''WARP3D: Dynamic Nonlinear Analysis of Solids Using a Preconditioned Conjugate Gradient Software Architecture," *Structural Research Series (SRS) 596*. UILU-ENG-94-2017. University of Illinois at Urbana-Champaign.

National Energy Boarding (NEB), 1996, "Stress Corrosion Cracking on Canadian Oil and Gas Pipelines", Report MH-2-95, Calgary.

Petrobrás, 2002, "*R*-Curve Measurements Using the Direct Potential Method for an API Grade 5L X60 Pipeline Steel," *Private Report* (in Portuguese).

Saxena, A., 1998, "Nonlinear Fracture Mechanics for Engineers", CRC Press, Boca Raton.

Silva, L. A. L., Cravero, S. and Ruggieri, C., 2006, "Correlation of Fracture Behavior in High Pressure Pipelines with Axial Flaws Using Constraint Designed Test Specimens - Part II: 3-D Effects on Constraint," *Engineering Fracture Mechanics*, Vol. 73, pp. 2123-2138.

Sumpter, J. D. G. and Turner, C. E., 1976, "Method for Laboratory Determination of J_c," Cracks and Fracture, ASTM STP 601, American Society for Testing and Materials, pp 3-18.

Zerbst, U., Ainsworth, R. A. and Schwalbe, K.-H., 2000, "Basic Principles of Analytical Flaw Assessment Methods", *International Journal of Pressure Vessels and Piping*, Vol. 77, pp. 855-867.

9. RESPONSIBILITY NOTICE

The authors are the only responsible for the printed material included in this paper.